

Geophysical Research Letters®



RESEARCH LETTER

10.1029/2025GL115335

Observing Ocean-Atmosphere Fluxes From Autonomous Surface Vehicles

Laurent Grare¹ , Luc Lenain¹ , and J. Thomas Farrar² 

¹Scripps Institution of Oceanography, University of California San Diego, La Jolla, CA, USA, ²Department of Physical Oceanography, Woods Hole Oceanographic Institution, Woods Hole, MA, USA

Key Points:

- Direct comparison and validation of atmospheric bulk properties collected from autonomous surface vehicles at 1 m above the ocean surface
- Measurements close to the ocean surface made from autonomous platforms can be used to reliably estimate bulk ocean-atmosphere fluxes
- At high winds, wave effects on the airflow close to the surface are either negligible or implicitly parameterized in the bulk algorithms

Supporting Information:

Supporting Information may be found in the online version of this article.

Correspondence to:

L. Grare,
lgrare@ucsd.edu

Citation:

Grare, L., Lenain, L., & Farrar, J. T. (2025). Observing ocean-atmosphere fluxes from autonomous surface vehicles. *Geophysical Research Letters*, 52, e2025GL115335. <https://doi.org/10.1029/2025GL115335>

Received 13 FEB 2025

Accepted 7 JUN 2025

Author Contributions:

Conceptualization: Laurent Grare, Luc Lenain, J. Thomas Farrar
Data curation: Laurent Grare
Formal analysis: Laurent Grare
Funding acquisition: Luc Lenain
Investigation: Laurent Grare, Luc Lenain, J. Thomas Farrar
Methodology: Laurent Grare, Luc Lenain, J. Thomas Farrar
Resources: Luc Lenain
Software: Laurent Grare
Supervision: Luc Lenain, J. Thomas Farrar
Validation: Laurent Grare, Luc Lenain, J. Thomas Farrar
Visualization: Laurent Grare, Luc Lenain, J. Thomas Farrar

Abstract With the increasing use of autonomous surface vehicles (ASVs) to characterize the marine atmospheric boundary layer, better understanding and evaluation of the observations collected from these platforms is needed. We present here unique comparisons of measurements of bulk properties and air-sea fluxes collected from ASVs right above the sea surface to state-of-the-art observations from R/P FLIP over a broad range of environmental conditions. We find good agreement between the two platforms, suggesting that near surface observations from such wave following vehicles are suitable to estimate air-sea fluxes using bulk formulas. This result is somewhat surprising, because the relatively low measurement height (1 m) is often below the wave crests. Possible interpretations are that the presence of waves does not violate the assumptions of the Monin-Obukhov theory inherent in the TOGA COARE bulk flux formulas, or that the empirical fit of the Monin-Obukhov stability functions somehow accounts for the wave effects.

Plain Language Summary Understanding the exchanges (fluxes) of energy, heat and mass at the ocean-atmosphere interface is crucial to characterize the coupling between the ocean and the atmosphere. With the increasing use of autonomous surface vehicles (ASV) that measure these exchanges at low heights (about 1 m) compared to traditional measurements from for example research vessels performed at higher heights (greater than 10 m), it is critical to evaluate the accuracy of such ASVs measurements. In this study, we compared fluxes measured from two Wave Gliders ASVs against those observed from the state-of-the-art research platform FLIP. For both platforms, the ocean-atmosphere exchanges were estimated using bulk algorithms derived from direct measurements of the wind and the atmospheric temperature and humidity. Estimates from the Wave Gliders were in good agreement (less than a few percent) with those from R/P FLIP, especially in the moderate wind regime. At low and high wind regimes, we observe higher differences which remain within a traditional range of accuracy defined by the scientific community ($\pm 10 \text{ W m}^{-2}$ for the heat flux estimates). These results are important for the community as it demonstrates that ASVs are capable of providing reliable estimates of the ocean-atmosphere exchanges.

1. Introduction

There has been growing recognition from both the traditional oceanographic and atmospheric science communities that to better understand and model the coupling between the atmosphere and the ocean, we need to drastically increase the density and spatial coverage of observations of air-sea fluxes (Cronin et al., 2019; Paterson et al., 2025). Autonomous surface vehicles (ASVs) have great potential to reduce the cost of making measurements at sea and for operation in arrays to measure spatial gradients of surface meteorology and air-sea interaction. They are also less prone to flow distortion than measurements collected from traditional research vessels (Edson et al., 1998; Gentemann et al., 2020; O'Sullivan et al., 2015; Popinet et al., 2004; Reeves Eyre et al., 2023; Ricciardulli et al., 2025; Yelland et al., 1998, 2002; Zhang et al., 2019). Some of these platforms, like the Wave Gliders discussed here, are physically constrained to collect atmospheric measurements close to the sea surface, often at a height of approximately 1 m, raising the question of how surface waves affect their meteorological measurements. Two of the most pressing questions are:

1. Can these platforms provide information equivalent to measurements from more traditional platforms, like buoys or ships, even though they are making measurements at heights that are often between wave crests and troughs?
2. As these small platforms are strongly influenced by the waves (and in the case of Wave Gliders, being propelled by waves), what are the measurement errors associated with the wave-induced motions?

© 2025. The Author(s).

This is an open access article under the terms of the [Creative Commons Attribution License](https://creativecommons.org/licenses/by/4.0/), which permits use, distribution and reproduction in any medium, provided the original work is properly cited.

Writing – original draft: Laurent Grare,
Luc Lenain, J. Thomas Farrar
Writing – review & editing:
Laurent Grare

From a reading of research from the last few decades on the shear and stratification in the marine atmospheric boundary layer (MABL), the answer to the first question would appear to be “probably not.” There is a fairly large body of literature on the “wave boundary layer” (Chalikov & Makin, 1991), a region extending some fraction of a wavelength above the sea surface, where waves modify the wind profile and violate the assumptions of the Monin-Obukhov theory that is fundamental to modern bulk flux formulas (Edson & Fairall, 1998; Vickers & Mahrt, 1999). The case is particularly strong for modification of the wind profile in old seas (when the waves move faster than the wind) or when the wind and swell are misaligned (Smedman et al., 1999; Vickers & Mahrt, 1999). What is less clear, though, is whether the waves generally modify the wind profile in an important way, especially in more common, fully developed seas. A more recent theoretical study by T. Hristov & Ruiz-Plancarte (2014) suggests that the modification of the wind profile by waves should be relatively small (a few percent of the wind speed) and difficult to measure. An additional complication is that the nondimensional shear and stratification profiles used in bulk flux algorithms are empirically determined, and so they may already compensate for wave effects.

We aim here to understand the extent to which measurements made from Wave Gliders and other platforms close to the surface (i.e., less than 2 m above the surface) can be used to reliably estimate momentum, heat and water vapor fluxes using bulk flux algorithms (Edson et al., 2013; Fairall et al., 2003). To address these questions, we revisit data from a field experiment with simultaneous and collocated MABL and flux measurements from two types of platforms, Wave Gliders and the Research Platform FLIP (R/P FLIP) across a broad range of environmental conditions (wind speed from 0 to 18 m s⁻¹ and significant wave height ranging from 1 to 4.5 m). Bulk atmospheric measurements from the Wave Gliders were collected at 1 m above the sea surface, and high-quality meteorological measurements were collected at 8 and 14 m on R/P FLIP, a platform specifically designed to reduce the influence of waves and flow distortion on meteorological measurements.

Overall, we find levels of agreement between the two types of platforms that, with root-mean-square differences on the order of 5 W m⁻² for sensible and latent heat flux, are comparable to the accuracy of long-term average of heat flux components and wind stress from state-of-the-art in situ observational methods (Cronin et al., 2019) and the World Meteorological Organization Global Climate Observing System goals (GCOS, 2025, pp. 119–120). This suggests that near surface observations from ASVs like the Wave Glider platforms are suitable for estimating ocean-atmosphere fluxes using bulk parameterizations, despite some differences found at low and high wind conditions that are discussed here.

2. Experiment

The data were collected as part of the Office Naval Research (ONR) funded Langmuir Cell Departmental Research Initiative (LCDRI) experiment conducted off the coast of Southern California in spring 2017. Two SV2 Wave Gliders operating in close proximity to the R/P FLIP were deployed for 16 days (Figure 1). Both the R/P FLIP and Wave Glider measurements from this experiment are also described in Grare et al. (2021).

The R/P FLIP is a 308-m long floating instrument platform that was designed to pitch backward by 90° so that its bow can point straight up with only about the front 17 m of the vessel above the water (Figure 1). In this configuration, it behaves like a spar buoy and is insensitive to most wave action. As part of the ONR LCDRI experiment, meteorological masts were installed on the portboard boom, equipped with Gill R3-50 sonic anemometers, Campbell Scientific HC2S3 temperature/humidity sensors, Novatel SPAN-CPT Global Positioning System (GPS)/Inertial Motion Unit (IMU) and XSENS MTI-300 IMUs near 8.3 ± 0.3 m and 14 ± 0.3 m above the mean sea level. Although the wave motion of the instruments was small, we used the GPS/IMU and the IMUs to motion-correct the anemometer measurements following Edson et al. (1998).

The Wave Gliders were equipped to measure bulk fluxes and atmospheric variables (wind, temperature, humidity) using a Vaisala WXT536 weather station mounted on a mast 1 m above the sea surface. The instrument was entirely repackaged to withstand intermittent submersion during capsizing (Grare, Statom, & Lenain, 2025). The Wave Gliders also were equipped with a dual-antenna Hemisphere Vector V104 GPS Compass which provided estimates of the position, linear velocity and heading at 1 and 10 Hz. Both Wave Gliders maintained rectangular patterns around R/P FLIP. Wave Glider Kelvin had a minimum, mean, and maximum separation of 150, 800, and 3,100 m, respectively while Wave Glider Pascal maintained a separation with R/P FLIP with a minimum, mean, and maximum separation of 230, 780, and 4,650 m, respectively.

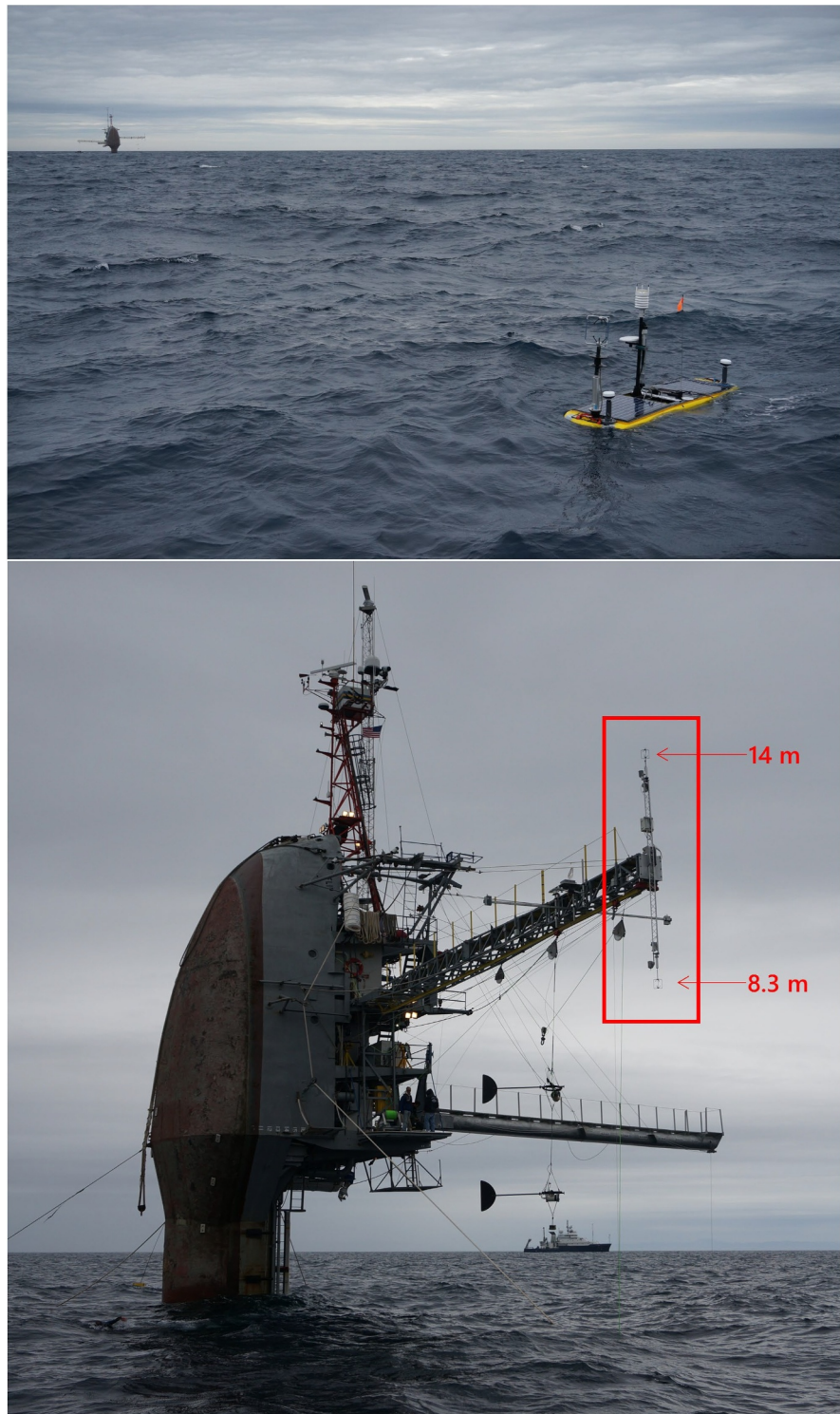


Figure 1. Upper panel: Wave Glider Pascal near R/P FLIP shortly after its deployment during the Langmuir Cell Departmental Research Initiative experiment. Lower panel: the R/P FLIP in its spar position, with the deployment positions of the Gill R3-50 sonic anemometers and Campbell Scientific HC2S3 temperature/humidity sensors on the meteorological boom.

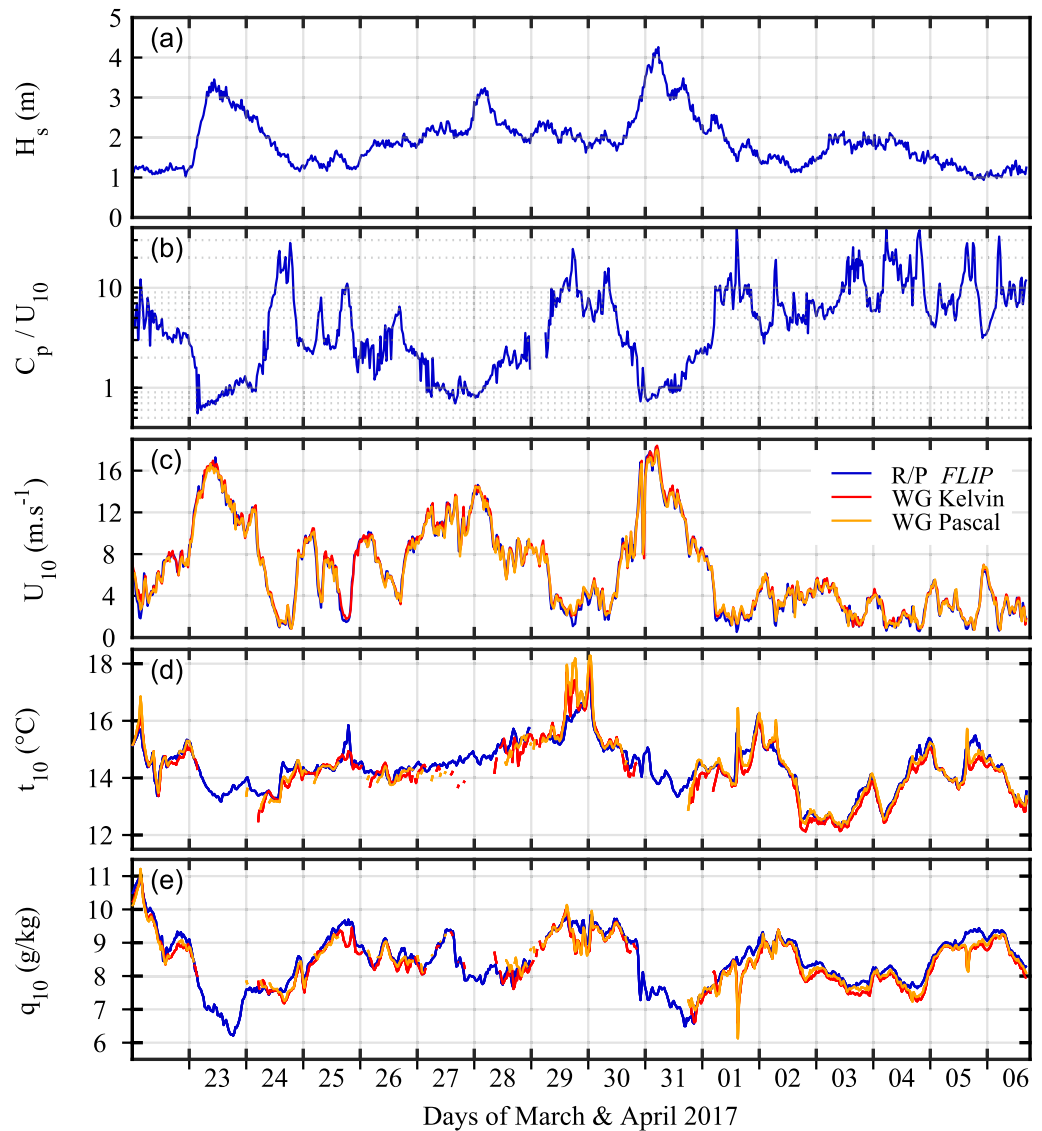


Figure 2. Time series of the (a) significant wave height H_s , (b) wave age C_p/U_{10} , (c) wind speed at 10 m U_{10} , (d) atmospheric temperature at 10 m t_{10} and (e) specific humidity at 10 m q_{10} from measurements performed on R/P FLIP at 8.3 m (blue) and from the two Wave Gliders Kelvin (red) and Pascal (orange) at 1 m. Bad temperature and humidity measurements from the Wave Gliders caused by capsizes at high winds/seas have been discarded.

3. Results

Figure 2 shows the time series of the significant wave height H_s , wave age C_p/U_{10} , and estimates at 10 m of the mean wind speed U_{10} , atmospheric temperature t_{10} and specific humidity q_{10} . Hereinafter temporal averaged values and their derived bulk properties were computed over a 30-min long window. In the top two panels, data from R/P FLIP only are reported while for the last three panels, data from the two Wave Gliders Kelvin and Pascal are plotted (red and orange) along with the data from R/P FLIP (blue). The range of environmental conditions was broad, with significant wave height reaching up to 4.5 m, wind speed from between 0.5 and 18 m s⁻¹ and wave age C_p/U_{10} ranging from 0.5 (strongly forced wind-waves regime) to 40 (wave driven wind regime). For all platforms, the 10-m estimates are computed using the Tropical Ocean-Global Atmosphere (TOGA) Coupled Ocean-Atmosphere Response Experiment (COARE) algorithm version 3.5 (Edson et al., 2013; Fairall et al., 2003), implementing the cool skin calculation but not the warm layer one. The velocity roughness model uses the new wind speed-dependent parameterization of the Charnock parameter $\alpha = mU_{10n} + b$ (Edson et al., 2013). In

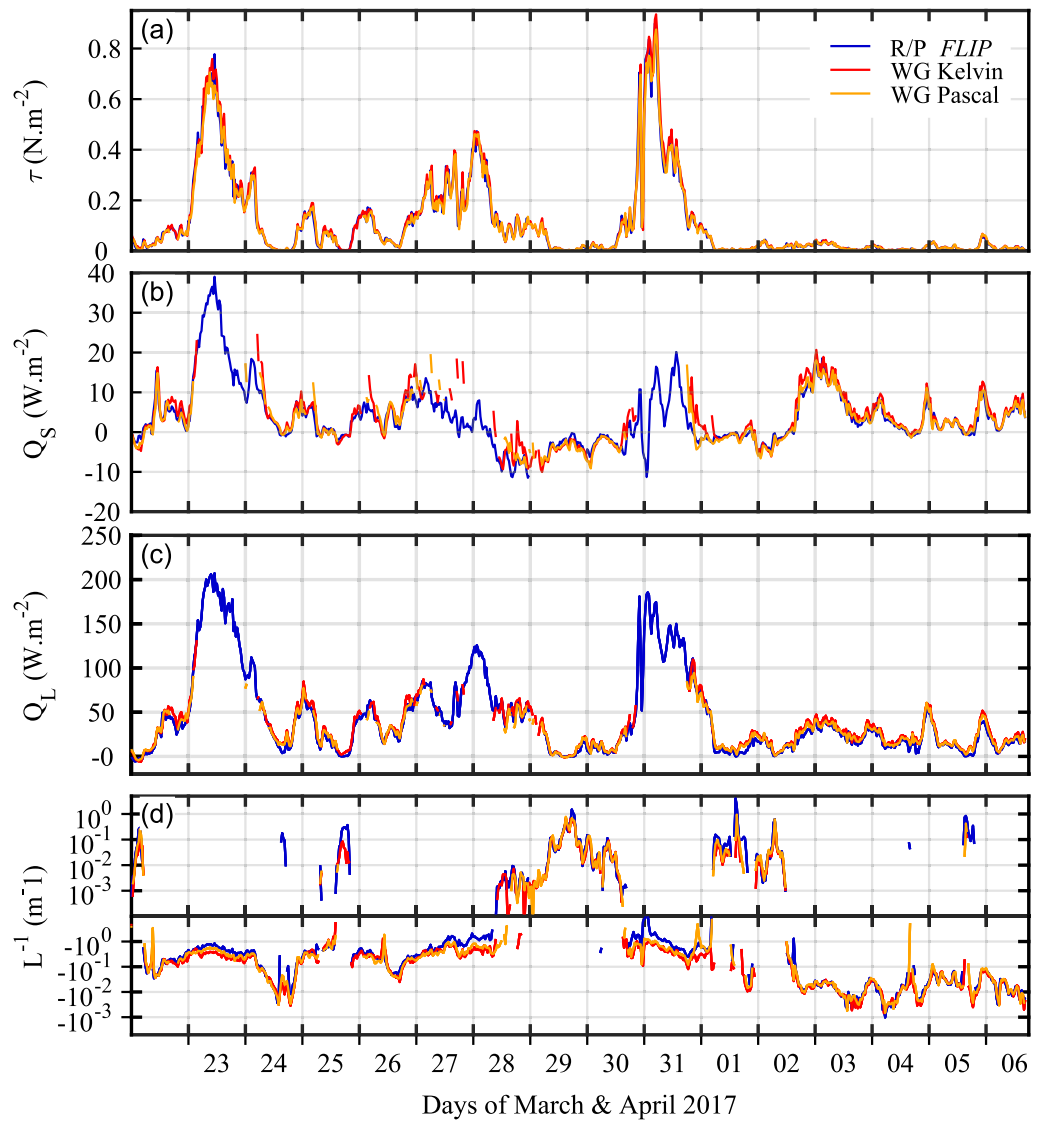


Figure 3. Time series of the (a) momentum flux τ , (b) sensible heat flux Q_S , (c) latent heat flux Q_L and (d) inverse of the Monin-Obukhov length L^{-1} measured on R/P FLIP at 8.3 m (blue) and by the two Wave Gliders Kelvin (red) and Pascal (orange) at 1 m. Corrupted sensible and latent heat flux measurements from the Wave Gliders caused by capsizes at high winds/seas have been discarded.

panel Figure 2c, the wind speed extrapolated at 10 m from the two Wave Gliders is in very good agreement with the data from R/P FLIP. For the temperature and the specific humidity extrapolated to 10 m, the comparison is not as good, though still capturing the general trend and temporal variability. Note that the temperature and humidity records from the Wave Gliders at high winds were removed from the analysis as they were contaminated by intermittent submersion of the instrument as, unlike the newer SV3 model, the SV2 Wave Gliders are prone to capsizing in high sea states. Capsize events were defined as instances in which the GPS receiver experienced a complete loss of satellite signal, indicative of submersion of the GPS antenna. Although wind measurements are unavailable during these periods, the wind sensor typically resumes normal operation shortly, that is few seconds, after the vehicle position is restored. In contrast, the atmospheric temperature and humidity sensors exhibit a slower recovery time to the submersion, of the order of 15–30 min. To ensure data quality, all temperature and humidity measurements within a 30-min record containing any capsize event were conservatively excluded from analysis.

Figure 3 presents estimates of the atmospheric momentum flux τ , the sensible heat flux Q_S , the latent heat flux Q_L and the inverse of the Monin-Obukhov length L^{-1} measured from R/P FLIP and the two Wave Gliders. As for Figure 2, Wave Glider variables derived from the temperature and humidity measurements have been discarded during capsizing. The momentum fluxes (Figure 3a) measured from R/P FLIP and Wave Gliders are in very good agreement. The sensible and latent heat fluxes are also in very good agreement for both types of platforms, demonstrating Wave Gliders ability to provide good estimates of the height and stability of the MABL.

Figure 4 presents scatter plots comparing bulk estimates from the Wave Gliders against those from R/P FLIP. The 10-m estimates U_{10} , t_{10} and q_{10} are plotted in the left column while the bulk flux estimates τ , Q_S and Q_L are shown in the right column. For each subplot, the small gray dots represent the estimates for each 30-min average, the large red dots are bin-averages, the dashed black line is the 1:1 ($y = x$) relationship and the dash-dotted blue line is the best linear fit of the data. The linear coefficients (slope and intercept) of this fit are reported in the bottom right corners along with its associated coefficient of determination r^2 and its root mean square error $rmse$.

For the wind speed at 10 m U_{10} (Figure 4a), the agreement between the R/P FLIP and Wave Gliders estimates is very good with a high coefficient of determination $r^2 = 0.983$ and $rmse$ around $0.5 \text{ W m}^{-2} \text{ m s}^{-1}$. The linear fit has a slope of 0.97 and a y-intercept of 0.29 m s^{-1} which could be due to an overestimation of U_{10} by the Wave Gliders at low winds. Figure 4c displays the relationship for t_{10} . The agreement is also encouraging, as the linear regressions have a r^2 close to 0.9, a slope slightly over one (1.07), and a negative y-intercept. Figure 4e displays the relationship for the specific humidity q_{10} . The comments above for the t_{10} measurements also apply to q_{10} with r^2 close to 0.9, but this time with the slope of the linear regression below one (0.92) and a positive y-intercept which is due to underestimates from the Wave Gliders for high values of the humidity. Note that if the linear regressions are constrained with a zero y-intercept, their slopes reach 1 ± 0.02 for all 10-m variables while their r^2 and $rmse$ values remain nearly constant. In Figure 4b, the estimates of τ are in very good agreement. The linear fit has a slope of 1.005, a y-intercept of 0.002 N m^{-2} , a $rmse$ of 0.027 N m^{-2} and $r^2 = 0.974$. For the sensible (Figure 4d) and latent heat (Figure 4f) fluxes, the slopes of the linear interpolation are 1.09 and 0.91 respectively with an overall overestimation of the sensible heat flux and underestimation of the latent heat flux when measured by the Wave Gliders. Visually, the spread looks larger for the sensible heat flux but this is a scale effect as the range of the sensible heat flux is much smaller than the latent heat flux range ($0\text{--}30 \text{ W m}^{-2}$ vs. $0\text{--}150 \text{ W m}^{-2}$). This is emphasized by the values of the $rmse$, 3.08 and 4.69 W m^{-2} , respectively.

4. Discussion

In Figure 5, the deviations between the Wave Gliders and R/P FLIP bulk estimates are presented for U_{10} , t_{10} , q_{10} and u_* (panels a, b, c, and d) using the ratio of the Wave Glider estimates over the R/P FLIP ones (e.g., $U_{10}^{WG}/U_{10}^{FLIP}$). For the sensible and latent heat fluxes, their absolute difference (e.g., $\Delta Q_S = Q_S^{WG} - Q_S^{FLIP}$) is presented in the panels (e) and (f) to account for the fact that the R/P FLIP heat fluxes can be null. For each subplot, the solid gray circles represent the estimates for each 30-min average discarding possible capsize events in panels (c) to (f) and the large red solid circles are their bin-averages. In the panel (a), the blue line represents the linear fit from Figure 4a expressed in the form $U_{10}^{WG}/U_{10}^{FLIP} = 0.97 + 0.29/U_{10}^{FLIP}$.

4.1. Surface Winds

Bin-average estimates agree with each other within a 5% margin for winds greater than 3 m s^{-1} for U_{10} and τ . Larger deviations occur at low winds. The agreement is especially very good in the high wind regime.

In the low wind regime, while the spread is larger, bin-average products suggest an overall over-estimation by the Wave Gliders measurements. This can be explained by wind profiles deviating from the Monin-Obukhov similarity theory in that wind regime. This spread has been both observed and modeled for swell dominated sea states with upward (ocean-to-atmosphere) momentum flux in the presence of low level wind jets (Grachev & Fairall, 2001; Hanley & Belcher, 2008; Högström et al., 2008, 2009, 2013, 2015; Semedo et al., 2009; Smedman et al., 2009; Sullivan et al., 2008). The large spread in the magnitude of these observations has been reported in previous studies, for example the large scatter of drag coefficient C_d versus U_{10} found at low winds (Drennan et al., 2003, 2007; Edson et al., 2013).

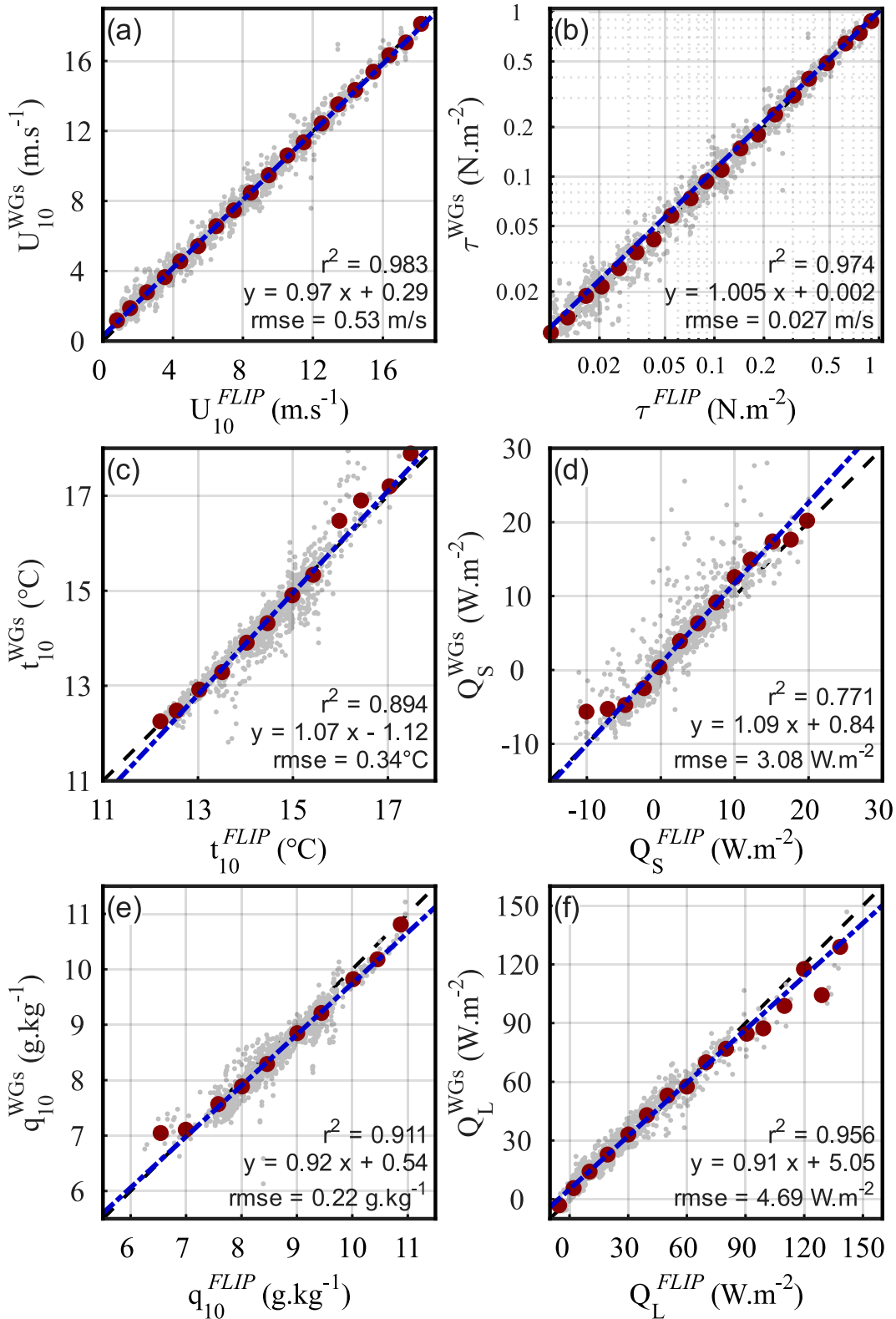


Figure 4. Scatter plots of the Wave Glider versus R/P FLIP relationship for (a) wind speed at 10 m U_{10} , (b) momentum flux τ (using logarithmic axes), (c) atmospheric temperature at 10 m t_{10} , (d) sensible heat flux Q_S , (e) specific humidity at 10 m q_{10} and (f) latent heat flux Q_L . X-axes correspond to the 8.3-m height R/P FLIP data while Y-axes correspond to the combined 1-m height data from the two Wave Gliders Kelvin and Pascal. Light gray dots are the 30-min averages (without capsizing data for panels (c) to (f)), large red dots are bin-averages. Dashed black line is the 1:1 line and the dash-dotted blue line is the best linear fit.

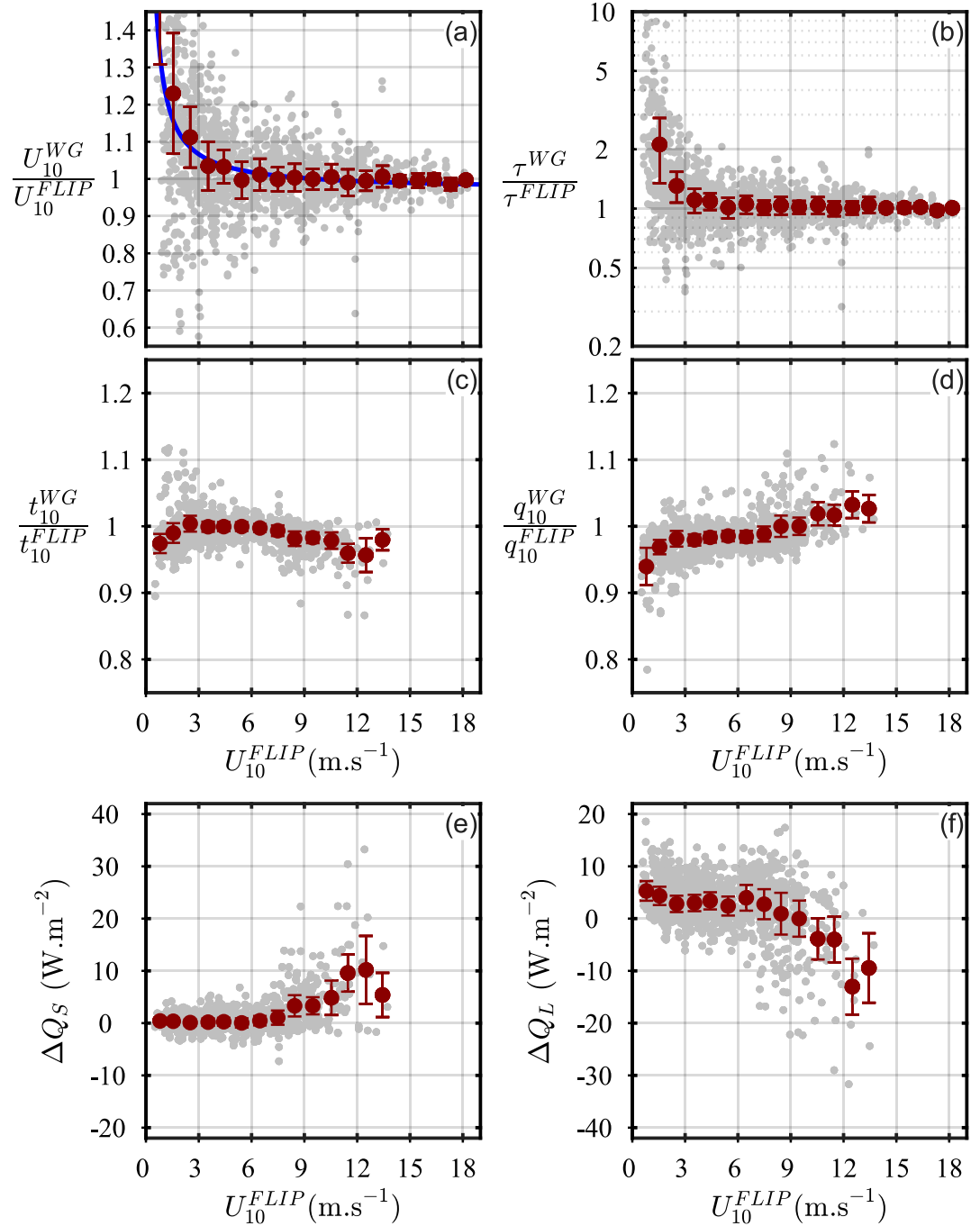


Figure 5. Evolution of the discrepancies between the Wave Gliders and R/P FLIP data as a function of the wind speed. Ratio of Wave Gliders over R/P FLIP data for the (a) wind speed at 10 m U_{10} , (b) momentum flux τ , (c) atmospheric temperature at 10 m t_{10} , and (d) ratio of the specific humidity at 10 m q_{10} . Difference between the Wave Gliders and R/P FLIP data for the (e) sensible heat flux Q_s and (f) latent heat flux Q_L . X-axes corresponds to the wind speed at 10 m U_{10} computed from the 8.3-m height R/P FLIP data. Small solid gray circles are the 30-min averaged and large red circle are the bin-averaged products. Bad measurements from the Wave Gliders caused by capsizes at high winds/seas have been discarded in panels (c) to (f). In panel (a), the blue line represents the linear fit from Figure 4a.

In the moderate and high wind regimes, Wave Gliders estimates agree surprisingly well with R/P FLIP estimates. One might expect that the Wave Glider measurements, collected at a height that is often below the wave crests, would be affected by the wave momentum flux (Chalikov & Makin, 1991; Vickers & Mahrt, 1999) and deviate

significantly from measurements outside the wave boundary layer. However, recent studies do not support this hypothesis. T. Hristov & Ruiz-Plancarte (2014) argues that the wave effect on the wind profile should be generally small. In addition, Carpenter et al. (2022); Grare et al. (2013, 2018); T. S. Hristov et al. (2003); Yousefi et al. (2020) have further demonstrated that the critical layer theory from Miles (1957) can accurately estimate the height of the wave boundary layer. Contrary to the approach where the thickness of the wave boundary layer is only defined by the wavelength of the dominant waves, the critical layer theory assumes that the wave effect vanishes above the critical height z_c where the wind speed $U(z_c)$ is equal to the wave speed c . This implies that the wave boundary layer does not depend on the wavelength of the dominant waves but rather on the ratio of the wave phase speed to the wind speed at any given height. It also implies that a wave boundary layer exists for each wave component from the surface up to its specific critical height $z_c(c)$. This is particularly relevant to the high wind regime where the critical layer height is very close to the surface for the shortest waves while the contribution from the longer waves decays slowly with height. Finally, another reason that could explain the good agreement between the Wave Glider and R/P FLIP estimates is that wave effects might be indirectly included in the COARE algorithm, as it relies on experimental data to constraint the parameterization. In that regard, we found that COARE version 3.5 performs much better than the previous 3.0 version, especially at high winds (see Figure S1 in Supporting Information S1). A major difference between the two versions is the inclusion of field observations collected at lower heights (e.g., buoys) that lead to a better parameterization of the relationship between the roughness length z_0 and the friction velocity u_* (Edson et al., 2013). Note that Figure S1 in Supporting Information S1 also highlights that adding bulk wave effects does not improve the agreement between the Wave Glider and R/P FLIP estimates.

4.2. Humidity and Temperature

Panels (c) and (d) of Figure 5 show that Wave Gliders observations of both the 10 m temperature and humidity are slightly underestimated (about 5%) in the low wind regime, are in very good agreement in the moderate regime and deviate again from the R/P FLIP estimates as the winds increase further ($U_{10} > 9 \text{ m s}^{-1}$), Wave Glider estimates of t_{10} being underestimated and q_{10} overestimated. These differences at high winds could be explained by the increasing density of sea spray in the MABL (Lenain & Melville, 2017; Veron, 2015) as the wind, and in turn breaking waves, ramps up. Since the concentration of sea spray decreases with height (Veron, 2015), Wave Gliders are expected to sample an atmosphere richer in sea spray aerosols, the sea spray generation layer, while observations from R/P FLIP are collected above, within the spray evaporative layer, which could explain these discrepancies. When sea spray aerosols are ejected from the ocean surface, they rapidly exchanges sensible heat with the atmosphere, reducing its temperature down to the dew point temperature which is lower than the surrounding atmospheric temperature (Veron, 2015, Figure 3). The cumulative effect of water droplets exhibiting this behavior could lead to atmospheric temperature measurements from Wave Gliders lower than measurements performed at heights with lower water droplets concentration (e.g., from R/P FLIP). These effects are qualitatively consistent with the differences observed in Figures 5c and 5d. Wetting of the temperature sensor during capsizing events could potentially also contribute to these differences at higher wind speeds. Note, while the earlier version of the Wave Glider vehicle used here (model SV2) is prone to capsizing, the newer SV3 version of the vehicle is much more stable and hardly capsizes for the range of environmental conditions considered here.

5. Summary

In this work, we have shown that bulk estimates of atmospheric variables (wind speed, temperature and humidity) and their derived bulk fluxes computed from ASV measurements collected at 1 m above the surface are in good agreement with state-of-art measurement performed at 8.3 m from R/P FLIP. The agreement is best in the moderate-wind regime where the bulk estimates are within a few percent and sensible and latent heat fluxes are within $\pm 5 \text{ W m}^{-2}$. We find small differences at low and high winds for U_{10} and u_* and only at high winds for t_{10} , q_{10} and their derived heat fluxes. Temperature and humidity differences can be explained by the presence of sea spray at high winds. Overall, the results presented here suggest that the modification of the wind profile by waves is small, consistent with the work of T. Hristov & Ruiz-Plancarte (2014). Since the non-dimensional shear and stratification profiles used in bulk flux algorithms (here with TOGA COARE 3.5) are empirically determined, it is likely that the derived fluxes products are already compensate for wave effects, which explains the good agreement found in fluxes and bulk atmospheric observations collected from R/P FLIP and Wave gliders.

We find that the absolute difference in the estimates of the sensible and latent heat fluxes presented in Figures 5e and 5f show that the Wave Gliders estimates are within $\pm 10\%$ of those from R/P FLIP for winds below 12 m s^{-1} , one of the original requirements of the TOGA COARE program. The measurements reported here from R/P FLIP are state-of-the-art, bulk meteorological measurements, made above the wave boundary layer, and the bulk flux estimates from the Wave Gliders agree to within the accuracies for other state-of-the-art bulk and direct flux measurements (e.g. Cronin et al., 2019, their Table 2). This further demonstrates the potential use of ASVs for contributing to the large scale, global air-sea fluxes observational network to augment more traditional observational platforms (ships, buoys and remote sensing).

Data Availability Statement

All presented data are found at the UCSD Library Digital Collection, <https://doi.org/10.6075/J0H41RS8> (Grare, Lenain, & Farrar, 2025).

References

- Carpenter, J., Buckley, M., & Veron, F. (2022). Evidence of the critical layer mechanism in growing wind waves. *Journal of Fluid Mechanics*, 948, A26. <https://doi.org/10.1017/jfm.2022.714>
- Chalikov, D., & Makin, V. (1991). Models of the wave boundary layer. *Boundary-Layer Meteorology*, 56(1), 83–99. <https://doi.org/10.1007/BF00119963>
- Cronin, M. F., Gentemann, C. L., Edson, J., Ueki, I., Bourassa, M., Brown, S., et al. (2019). Air-sea fluxes with a focus on heat and momentum. *Frontiers in Marine Science*, 6. <https://doi.org/10.3389/fmars.2019.00430>
- Drennan, W. M., Graber, H. C., Hauser, D., & Quentin, C. (2003). On the wave age dependence of wind stress over pure wind seas. *Journal of Geophysical Research*, 108(C3), 8062. <https://doi.org/10.1029/2000JC000715>
- Drennan, W. M., Zhang, J. A., French, J. R., McCormick, C., & Black, P. G. (2007). Turbulent fluxes in the hurricane boundary layer. Part II: Latent heat flux. *Journal of the Atmospheric Sciences*, 64(4), 1103–1115. <https://doi.org/10.1175/JAS3889.1>
- Edson, J. B., & Fairall, C. W. (1998). Similarity relationships in the marine atmospheric surface layer for terms in the TKE and scalar variance budgets. *Journal of the Atmospheric Sciences*, 55(13), 2311–2328. [https://doi.org/10.1175/1520-0469\(1998\)055%3C2311:SRITMA%3E2.0.CO;2](https://doi.org/10.1175/1520-0469(1998)055%3C2311:SRITMA%3E2.0.CO;2)
- Edson, J. B., Hinton, A. A., Prada, K. E., Hare, J. E., & Fairall, C. W. (1998). Direct covariance flux estimates from mobile platforms at sea. *Journal of Atmospheric and Oceanic Technology*, 15, 547–562. [https://doi.org/10.1175/1520-0426\(1998\)015<0547:DCFEFM>2.0.CO;2](https://doi.org/10.1175/1520-0426(1998)015<0547:DCFEFM>2.0.CO;2)
- Edson, J. B., Jampana, V., Weller, R. A., Bigorre, S. P., Plueddemann, A. J., Fairall, C. W., et al. (2013). On the exchange of momentum over the open ocean. *Journal of Physical Oceanography*, 43(8), 1589–1610. <https://doi.org/10.1175/jpo-d-12-0173.1>
- Fairall, C. W., Bradley, E. F., Hare, J. E., Grachev, A. A., & Edson, J. B. (2003). Bulk parameterization of air–sea fluxes: Updates and verification for the coare algorithm. *Journal of Climate*, 16(4), 571–591. [https://doi.org/10.1175/1520-0442\(2003\)016<0571:BPOASF>2.0.CO;2](https://doi.org/10.1175/1520-0442(2003)016<0571:BPOASF>2.0.CO;2)
- GCOS. (2025). *The 2022 GCOS ECVs requirements (Technical Reports No. GCOS-245)*. World Meteorological Organization. Retrieved from <https://library.wmo.int/idurl/4/58111>
- Gentemann, C. L., Scott, J. P., Mazzini, P. L. F., Pianca, C., Akella, S., Minnett, P. J., et al. (2020). Saildrone: Adaptively sampling the marine environment. *Bulletin of the American Meteorological Society*, 101(6), E744–E762. <https://doi.org/10.1175/bams-d-19-0015.1>
- Grachev, A. A., & Fairall, C. W. (2001). Upward momentum transfer in the marine boundary layer. *Journal of Physical Oceanography*, 31(7), 1698–1711. [https://doi.org/10.1175/1520-0485\(2001\)031<1698:UMTITM>2.0.CO;2](https://doi.org/10.1175/1520-0485(2001)031<1698:UMTITM>2.0.CO;2)
- Grare, L., Lenain, L., & Farrar, J. T. (2025a). Observing ocean-atmosphere fluxes from autonomous surface vehicles [dataset]. *UC San Diego Library Digital Collections*. <https://doi.org/10.6075/J0H41RS8>
- Grare, L., Lenain, L., & Melville, W. K. (2013). Wave-coherent airflow and critical layers over ocean waves. *Journal of Physical Oceanography*, 43(10), 2156–2172. <https://doi.org/10.1175/JPO-D-13-056.1>
- Grare, L., Lenain, L., & Melville, W. K. (2018). Vertical profiles of the wave-induced airflow above ocean surface waves. *Journal of Physical Oceanography*, 48(12), 2901–2922. <https://doi.org/10.1175/JPO-D-18-0121.1>
- Grare, L., Statom, N., & Lenain, L. (2025b). Technical report: Waterproofing vaisala WXT520 and WXT530 meteorological sensors. *Zenodo*. <https://doi.org/10.5281/zenodo.15497989>
- Grare, L., Statom, N. M., Pizzo, N., & Lenain, L. (2021). Instrumented wave gliders for air-sea interaction and upper ocean research. *Frontiers in Marine Science*, 8, 888. <https://doi.org/10.3389/fmars.2021.664728>
- Hanley, K. E., & Belcher, S. E. (2008). Wave-driven wind jets in the marine atmospheric boundary layer. *Journal of the Atmospheric Sciences*, 65(8), 2646–2660. <https://doi.org/10.1175/2007JAS2562.1>
- Högström, U., Rutgersson, A., Sahlée, E., Smedman, A.-S., Hristov, T., Drennan, W., & Kahma, K. (2013). Air-sea interaction features in the Baltic Sea and at a Pacific trade-wind site: An inter-comparison study. *Boundary-Layer Meteorology*, 147(1), 139–163. <https://doi.org/10.1007/s10546-012-9776-8>
- Högström, U., Sahlée, E., Drennan, W. M., Kahma, K. K., Smedman, A. S., Johansson, C., et al. (2008). Momentum fluxes and wind gradients in the marine boundary layer: A multi platform study. *Boreal Environment Research*, 13, 475–502. Retrieved from <https://api.semanticscholar.org/CorpusID:29849803>
- Högström, U., Sahlée, E., Smedman, A.-S., Rutgersson, A., Nilsson, E., Kahma, K. K., & Drennan, W. M. (2015). Surface stress over the ocean in swell-dominated conditions during moderate winds. *Journal of the Atmospheric Sciences*, 72(12), 4777–4795. <https://doi.org/10.1175/JAS-D-15-0139.1>
- Högström, U., Smedman, A., Sahlée, E., Drennan, W. M., Kahma, K. K., Pettersson, H., & Zhang, F. (2009). The atmospheric boundary layer during swell: A field study and interpretation of the turbulent kinetic energy budget for high wave ages. *Journal of the Atmospheric Sciences*, 66(9), 2764–2779. <https://doi.org/10.1175/2009JAS2973.1>
- Hristov, T., & Ruiz-Plancarte, J. (2014). Dynamic balances in a wavy boundary layer. *Journal of Physical Oceanography*, 44(12), 3185–3194. <https://doi.org/10.1175/jpo-d-13-0209.1>

Acknowledgments

This research was supported by grants from the Physical Oceanography and Atmospheric programs at ONR (N00014-17-1-2171, N00014-14-1-0710, N00014-21-1-2825, N00014-23-1-2055, N00014-23-1-2045, and N00014-19-12635), NASA (80NSSC19K1688, 80NSSC19K1256, and 80NSSC23K0985), and NSF (OCE2219752). This work is a contribution to the S-MODE project, an EVS-3 Investigation awarded under NASA Research Announcement NNH17ZDA001N-EVS3.

- Hristov, T. S., Miller, S. D., & Friehe, C. A. (2003). Dynamical coupling of wind and ocean waves through wave-induced air flow. *Nature*, 422(6927), 55–58. <https://doi.org/10.1038/nature01382>
- Lenain, L., & Melville, W. K. (2017). Evidence of sea-state dependence of aerosol concentration in the marine atmospheric boundary layer. *Journal of Physical Oceanography*, 47(1), 69–84. <https://doi.org/10.1175/JPO-D-16-0058.1>
- Miles, J. W. (1957). On the generation of surface waves by shear flows. *Journal of Fluid Mechanics*, 3(2), 185–204. Retrieved from <https://www.cambridge.org/core/journals/journal-of-fluid-mechanics/article/on-the-generation-of-surface-waves-by-shear-flows/40B503619B6D4571BEF3D31CB8925084>
- O'Sullivan, N., Landwehr, S., & Ward, B. (2015). Air-flow distortion and wave interactions on research vessels: An experimental and numerical comparison. *Methods in Oceanography*, 12, 1–17. <https://doi.org/10.1016/j.mio.2015.03.001>
- Patterson, R. G., Cronin, M. F., Swart, S., Beja, J., Edholm, J. M., McKenna, J., et al. (2025). Uncrewed surface vehicles in the global ocean observing system: A new Frontier for observing and monitoring at the air-sea interface. *Frontiers in Marine Science*, 12. <https://doi.org/10.3389/fmars.2025.1523585>
- Popinet, S., Smith, M., & Stevens, C. (2004). Experimental and numerical study of the turbulence characteristics of airflow around a research vessel. *Journal of Atmospheric and Oceanic Technology*, 21(10), 1575–1589. [https://doi.org/10.1175/1520-0426\(2004\)021<1575:EANSOT>2.0.CO;2](https://doi.org/10.1175/1520-0426(2004)021<1575:EANSOT>2.0.CO;2)
- Reeves Eyre, J. E. J., Cronin, M. F., Zhang, D., Thompson, E. J., Fairall, C. W., & Edson, J. B. (2023). Saildrone direct covariance wind stress in various wind and current regimes of the tropical pacific. *Journal of Atmospheric and Oceanic Technology*, 40(4), 503–517. <https://doi.org/10.1175/jtech-d-22-0077.1>
- Ricciardulli, L., Manaster, A., & Lindsley, R. (2025). Investigation of a calibration change in the ocean surface wind measurements from the TAO buoy array. *Bulletin of the American Meteorological Society*, 106(2), E242–E260. <https://doi.org/10.1175/bams-d-24-0072.1>
- Semedo, A., Saetra, O., Rutgersson, A., Kahma, K. K., & Pettersson, H. (2009). Wave-induced wind in the marine boundary layer. *Journal of the Atmospheric Sciences*, 66(8), 2256–2271. <https://doi.org/10.1175/2009JAS3018.1>
- Smedman, A., Högström, U., Bergström, H., Rutgersson, A., Kahma, K. K., & Pettersson, H. (1999). A case study of air-sea interaction during swell conditions. *Journal of Geophysical Research*, 104(C11), 25833–25851. <https://doi.org/10.1029/1999JC900213>
- Smedman, A., Hogstrom, U., Sahlée, E., Drennan, W. M., Kahma, K. K., Pettersson, H., & Zhang, F. (2009). Observational study of marine atmospheric boundary layer characteristics during swell. *Journal of the Atmospheric Sciences*, 66(9), 2747–2763. <https://doi.org/10.1175/2009JAS2952.1>
- Sullivan, P. P., Edson, J. B., Hristov, T., & McWilliams, J. C. (2008). Large eddy simulations and observations of atmospheric marine boundary layers above non-equilibrium surface waves. *Journal of the Atmospheric Sciences*, 65(4), 1225–1245. <https://doi.org/10.1175/2007JAS2427.1>
- Veron, F. (2015). Ocean spray. *Annual Review of Fluid Mechanics*, 47(1), 507–538. <https://doi.org/10.1146/annurev-fluid-010814-014651>
- Vickers, D., & Mahrt, L. (1999). Observations of non-dimensional wind shear in the coastal zone. *Quarterly Journal of the Royal Meteorological Society*, 125(559), 2685–2702. <https://doi.org/10.1002/qj.49712555917>
- Yelland, M. J., Moat, B. I., Pascal, R. W., & Berry, D. I. (2002). Cfd model estimates of the airflow distortion over research ships and the impact on momentum flux measurements. *Journal of Atmospheric and Oceanic Technology*, 19(10), 1477–1499. [https://doi.org/10.1175/1520-0426\(2002\)019<1477:CMEOTA>2.0.CO;2](https://doi.org/10.1175/1520-0426(2002)019<1477:CMEOTA>2.0.CO;2)
- Yelland, M. J., Moat, B. I., Taylor, P. K., Pascal, R. W., Hutchings, J., & Cornell, V. C. (1998). Wind stress measurements from the open ocean corrected for airflow distortion by the ship. *Journal of Physical Oceanography*, 28(7), 1511–1526. [https://doi.org/10.1175/1520-0485\(1998\)028<1511:WSMFTO>2.0.CO;2](https://doi.org/10.1175/1520-0485(1998)028<1511:WSMFTO>2.0.CO;2)
- Yousefi, K., Veron, F., & Buckley, M. P. (2020). Momentum flux measurements in the airflow over wind-generated surface waves. *Journal of Fluid Mechanics*, 895, A15. <https://doi.org/10.1017/jfm.2020.276>
- Zhang, D., Cronin, M., Meing, C., Farrar, J. T., Jenkins, R., Peacock, D., et al. (2019). Comparing air-sea flux measurements from a new unmanned surface vehicle and proven platforms during the spurs-2 field campaign. *Oceanography*, 32(2), 122–133. <https://doi.org/10.5670/oceanog.2019.220>